OPTIMAL PUMP WAVELENGTH PLACEMENT IN LOSSLESS POLARIZATION ATTRACTION

Matteo Barozzi and Armando Vannucci
Dipartimento di Ingegneria dell'Informazione, Università degli Studi di Parma,
viale delle Scienze 181/A, 43124 Parma, Italy. Email: matteo.barozzi82@gmail.com

In lossless polarization attraction, we find the optimal (co-propagating) pump wavelength placement and the related scaling rule, as a function of symbol period. We demonstrate that polarization attraction occurs only within a limited range of walk-off values.

1. Introduction

Lossless polarization attraction (LPA) is a nonlinear phenomenon for which the arbitrary polarization of a signal, propagating in a fiber, is attracted towards the polarization of a continuous wave (CW) pump, that is usually counter-propagating. Being based on the Kerr effect, LPA is promising for devising polarization control devices and for other all-optical telecom applications. One of the possible applications of LPA is the noise cleaning of a polarized signal, which can enhance the OSNR by a factor close to 3 dB [1].
However, the numerical simulation of LPA requires costly iterative algorithms [2], due to the counter-propagating configuration. The study of LPA has recently moved to the co-propagating configuration [3], which is simpler to simulate and, mostly, even more flexible, since it allows the designer to finely control the relative pump-probe propagation speed, i.e., the *walk-off*, by selecting the fiber type and the pump-probe wavelength spacing $\Delta\lambda$ [3]. As a consequence, the co-propagating LPA can effectively repolarize even short (picoseconds) pulses, whereas LPA traditionally fails because of the large (microseconds) transient time [4].
Here, we characterize the performance of LPA, in the co-propagating configuration, as a function of the total walk-off delay T_D, for values of the pulse duration typical of telecom links (symbol period: $10\text{-}10^3$ ps). At the same time, we shall cast new light onto the central role of walk-off in the dynamics of LPA, by showing the interval of wavelengths where to place the pump, in order to reach the *polarization attraction regime*.

2. System Model and Parameters

We consider LPA occurring in a non-zero dispersion-shifted fiber (NZ-DSF) span, with length L=20 km, attenuation α=0.2 dB/km, nonlinear Kerr coefficient γ=1.99 $W^{-1}km^{-1}$ and dispersion parameter D=4 ps/nm/km. We inject into the fiber a single intensity-modulated pulse (probe) with limited duration T_S, placed at the fiber zero dispersion wavelength λ_{ZDW}. A fully-polarized CW pump, placed at wavelength λ_p, is injected into the same fiber end as the probe. Hence, pump and probe propagate at different speeds, and their total walk-off delay, at the fiber output, is $T_D=D\cdot\Delta\lambda\cdot L$, where $\Delta\lambda=\lambda_p-\lambda_{ZDW}$. Since we fix the fiber type and length, as well as the probe wavelength, T_D can be tuned by varying the pump wavelength placement. In order to explore a wide range of walk-off delays, we varied $\Delta\lambda$ from 0 to 20 nm, still keeping probe and pump within the conventional telecom bandwidth (*C-band*), so that T_D varies between 0 and 1600 ps. The simulation of very small T_D values is mainly of theoretical interest, since it would require $\Delta\lambda\cong0$, hence an overlap of pump and probe spectra [3].
We consider the practical case of a randomly birefringent telecom fiber, with a PMD coefficient D_{PMD}=0.05 ps·km$^{-0.5}$, typical of recently manufactured fibers. For the fiber length L used in our LPA, D_{PMD} is small enough to make linear PMD effects negligible [3], while the random birefringence is such that the propagation is governed by the Manakov equation [3,4]. Hence, the evolution of the (unattenuated) probe and pump Stokes vectors is governed by the following equations [3]:

$$\frac{\partial \boldsymbol{S}}{\partial z}+\frac{1}{2\mathrm{v}_{wo}}\frac{\partial \boldsymbol{S}}{\partial t}=\frac{8}{9}\gamma\,\mathrm{e}^{-\alpha z}\boldsymbol{P}\times\boldsymbol{S} \qquad \frac{\partial \boldsymbol{P}}{\partial z}-\frac{1}{2\mathrm{v}_{wo}}\frac{\partial \boldsymbol{P}}{\partial t}=\frac{8}{9}\gamma\,\mathrm{e}^{-\alpha z}\boldsymbol{S}\times\boldsymbol{P} \tag{1}$$

that are expressed in a time-frame moving at speed v_{ref}, where $2\mathrm{v}_{ref}^{-1}=v_s^{-1}+v_p^{-1}$ and $v_{s,p}$ are the group velocities at probe and pump wavelengths, so that $v_{wo}^{-1}=v_s^{-1}-v_p^{-1}$ is the inverse of the "walk-off speed". In (1), $\boldsymbol{S}(z,t)=S_0(z,t)\hat{\boldsymbol{s}}(z,t)$ is the probe Stokes vector, with magnitude $S_0(z,t)$, equal to the power profile of the probe pulse, and direction $\hat{\boldsymbol{s}}(z,t)$, representing the state of polarization (SOP) evolution, onto the Poincaré sphere; similarly, $\boldsymbol{P}(z,t)=P_0\,\hat{\boldsymbol{p}}(z,t)$ is the Stokes vector of the CW pump. The equations in (1) are spherically isotropic, implying that polarization attraction occurs for any input pump SOP $\hat{\boldsymbol{p}}(0)$ (fully polarized, at z=0) [2,3]. In the results that follow, we arbitrarily choose a linear horizontal pump polarization, hence $\hat{\boldsymbol{p}}(0)=\hat{\boldsymbol{s}}_1$ is the first Stokes axis.

When a fully polarized probe pulse, with a specific input SOP $\hat{\boldsymbol{s}}(0)$, is launched into the fiber, the LPA performance is quantified by the *degree of attraction* (DOA) [5]. Averaging the DOA over the (uniform) distribution of input probe SOPs, the overall performance of LPA coincides with the usual definition of the degree of polarization (DOP), evaluated over the output probe [3], $DOP=\|E[\langle\boldsymbol{S}(L,t)\rangle]\|/\langle S_0(L,t)\rangle$, where $\langle\cdot\rangle$ and $E[\cdot]$ represent time- and statistical-averaging, while $\|\cdot\|$ is the euclidean norm. To evaluate the DOP, we averaged over 100 launched probe SOPs, with uniform distribution over the Poincaré sphere. Being a nonlinear phenomenon, LPA depends mainly on the injected power level [3,5]. Here, we kept the overall optical power at a moderate level, and chose the same probe and pump peak power, $P_0=S_0^{peak}=200\,mW$. At such power levels, four wave mixing (FWM) effects, such as pump power depletion (that eqs. (1) do not account for) are negligible [3], as we numerically verified.

3. Optimization of the pump wavelength placement

Fig. 1(a) shows the LPA performance, quantified by the output DOP, as a function of the total walk-off delay T_D between pump and probe. Different plots are obtained for a rectangular probe pulse with the following durations T_S: 1000, 400, 100, and 10 ps. Fig. 1(a) shows that an optimal walk-off delay T_D^*, hence an optimal pump wavelength λ_p^*, exists, that maximizes the performance of attraction. While such optimal T_D^* (and the whole plot) depend on the probe pulse duration T_S, it is remarkable that the best DOP value is independent of it, being $DOP^*\cong0.78$ for all the tested pulses. Moreover, T_D^* increases with the pulse duration T_S, meaning that the effectiveness of polarization attraction fades away, i.e., DOP drops below DOP^*, whenever the walk-off delay T_D is too large or too small, compared with the duration of the pulse to be attracted.

The above results suggest that a scaling rule exists. This is indeed verified in Fig. 1(b), where the obtained DOP values are plotted versus the walk-off delay T_D/T_S, normalized to the pulse duration. Hence, each curve in Fig. 1(a) can be obtained by rescaling the single curve, visible in Fig. 1(b), which summarizes the performance of LPA for any pulse duration, at the chosen power level. In agreement with the results in [3], such a curve is expected to reach larger DOP values, by increasing pump and probe power, although we do not test other power levels, here. The optimal normalized walk-off delay is $T_D^*/T_S\cong1.75$.

The scaling rule, just verified numerically, should not surprise, since it can be demonstrated analytically. From the propagation equations (1), suppose we make the change of time scale $\tau=t/T$, so that $\boldsymbol{S}'(z,\tau)=\boldsymbol{S}(z,t/T)$ is a compressed version (if 0 < T < 1) of the probe pulse. It is easy to show that $\boldsymbol{S}'(z,\tau)$ and $\boldsymbol{P}'(z,\tau)=\boldsymbol{P}(z,t/T)$ obey a set of equations identical to (1), provided that the walk-off speed v_{wo} is changed into $v_{wo}'=v_{wo}T$. This implies that the output probe evolution, hence its polarization and the corresponding overall DOP, are the same as those got by solving (1), for a rescaled walk-off speed, hence for a rescaled delay $T_D'=L/v_{wo}'=T_D/T$. As a consequence, if we choose the time-scaling

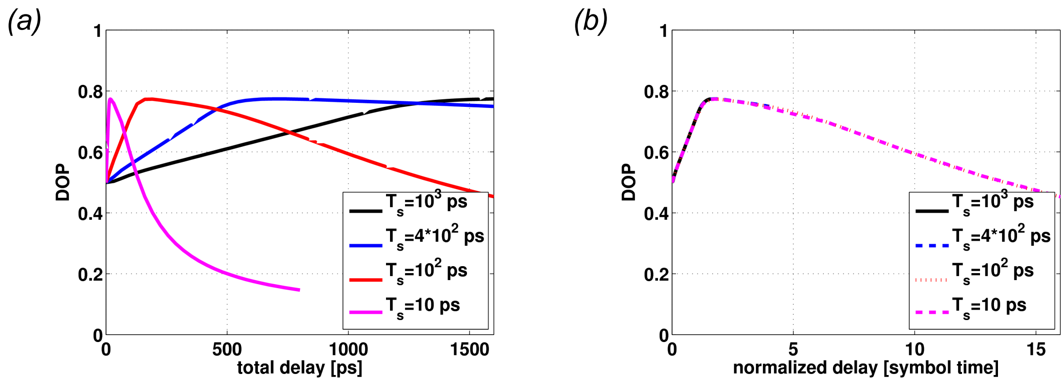

Fig.1 Performance of lossless polarization attraction (LPA): output probe DOP vs. total pump-probe walk-off delay T_D. Results obtained for different pulse durations T_S (a) obey a scaling law, so that DOP only depends on the normalized delay T_D/T_S (b).

factor equal to the pulse duration, $T=T_S$, all the curves in Fig. 1(a) coincide, as demonstrated in Fig. 1(b). The practical implication of the obtained result is that, given the LPA parameters and the pulse duration, the optimal $T_D^* \cong 1.75 \cdot T_S$ can be reached by placing the pump at an optimal wavelength distance $\Delta\lambda^* = T_D^*/(D \cdot L)$ from the probe. On the contrary, for a given pump wavelength, hence a fixed $\Delta\lambda$ (and T_D), an optimal pulse duration $T_S^* \cong T_D/1.75$ exists, that maximizes the effectiveness of LPA. In any case, polarization attraction effectively occurs only for a limited range of pulse durations; e.g., in the present case of system parameters, results in Fig. 1(b) show that $T_D/6 < T_S < T_D$ is required, in order to get DOP > 0.7.

4. Polarization Rotation and Polarization Attraction Regimes

As a matter of fact, lossless polarization attraction is the joint effect of Kerr nonlinearity and walk-off, both occurring between pump and probe, in carefully balanced amounts. Fig. 2 shows a numerical exemplification of this assertion.

The plots in Fig. 2 show the evolution of the probe polarization along the LPA fiber. Each (red) circle is the time-averaged SOP of the probe pulse, at a given position $0 \le z \le L$, i.e., the direction of $\overline{\boldsymbol{S}}(z) = \langle \boldsymbol{S}(z,t) \rangle$. Fig. 2 was obtained for specific probe and pump input SOPs: namely, $\hat{\boldsymbol{s}}(0) = \hat{\boldsymbol{s}}_3$ (right-circular) and $\hat{\boldsymbol{p}}(0) = \hat{\boldsymbol{s}}_1$ (linear-horizontal), both marked with a (red or black) vector, in the figure. The three plots correspond to different values of the walk-off delay T_D, equal to zero (a), $5 \cdot T_S$ (b), and $32 \cdot T_S$ (c).

As clearly seen in Fig. 2, the average probe SOP, starting at $\hat{\boldsymbol{s}}_3$, moves towards the pump SOP $\hat{\boldsymbol{s}}_1$, hence evolves according to a *polarization attraction regime*, only for the intermediate case. On the contrary, the probe SOP keeps rotating in a circle, i.e., undergoes a *polarization rotation regime*, in the other two cases. Such a behavior, that we regularly observed for any input probe SOP, can be simply explained, in the case T_D=0 (Fig. 2(a)). In fact, it is well known that, in the absence of walk-off, both pump and probe SOPs evolve in z according to a "carousel model" [6], i.e., they rotate around a fixed *pivot* equal to their vector sum, hence located middle way between $\hat{\boldsymbol{s}}_3$ and $\hat{\boldsymbol{s}}_1$, in the present case of equal pump and probe power. The circle thus described by $\overline{\boldsymbol{S}}(z)$, as seen in Fig. 2(a) can even become aligned with the pump SOP ($\hat{\boldsymbol{s}}_1$), for certain values of z and/or power, but still in a *polarization rotation regime,* and not in the *polarization attraction regime*, hence subject to change with length, power, and input probe SOP. The other extreme case of very large walk-off, shown in Fig. 2(c), can be equally well explained with the rotation of the probe SOP around the pump SOP (here $\hat{\boldsymbol{s}}_1$), as dictated by the first eq. in (1). This case differs from the zero walk-off case since, in the limit, it is as if the probe pulse were infinitely short, hence is unable to perturb the pump polarization, through the second eq. in (1).

Hence, the two *polarization rotation regimes* can be explained theoretically and never result

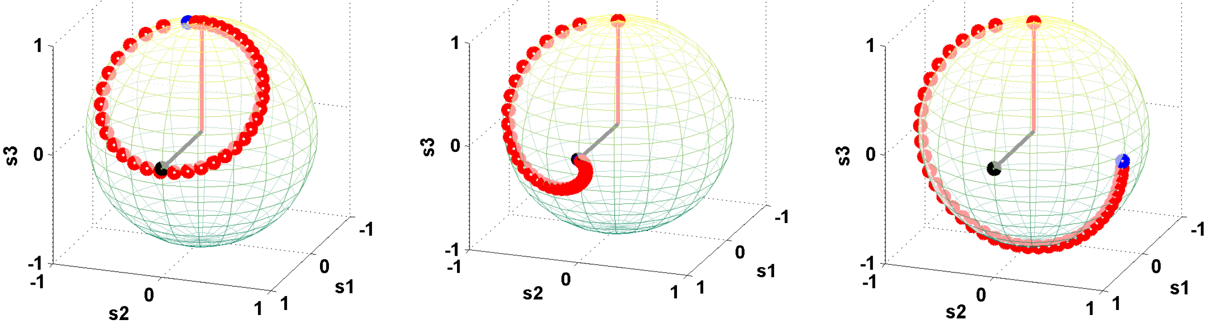

(a) *(b)* *(c)*

Fig.2 Evolution of the average probe pulse polarization along the LPA fiber. Here, the input probe and pump SOPs are right-circular and linear-horizontal ($\hat{s}_{3,1}$, as marked in the figure). A too small (a: T_D=0) or too large (c: T_D=32·T_S) walk-off induces polarization rotation, while LPA is effective for a intermediate values (b: T_D=5·T_S).

in polarization attraction, since the probe SOP evolves in circles (although an illusory attraction can occur, in the first case, for specific LPA parameters). An effective *polarization attraction regime* is reached, instead, for intermediate values of the walk off, close to the optimal T_D, that depend on the duration of the pulse to be attracted. In this case, the probe SOP $\bar{S}(z)$ follows a spiral trajectory, as in Fig. 2(b), leading towards the pump SOP, at the LPA output. The geometrical features of such a spiral, related to the polarization attraction dynamics, deserve further investigation.

5. Conclusion

We characterize the performance of lossless polarization attraction, in the co-propagating configuration, by measuring the average output DOP, as a function of the walk-off delay T_D between the attracting CW pump and an attracted probe pulse, with duration typical of telecom links. We demonstrate that a scaling rule exists, so that the optimal performance (DOP) can be achieved for any pulse duration, provided that the walk-off is tuned accordingly, by placing the pump at an optimal wavelength. As a consequence, we show that the "polarization attraction regime" occurs only when Kerr nonlinearity and walkoff are carefully balanced. In this case, the probe SOP evolves along a spiral trajectory, ideally collapsing into the pump SOP, while, in all other cases, we only observe a SOP rotation, that never results in a genuine polarization attraction.

Bibliography

[1] M. Barozzi, A. Vannucci, "A novel device to enhance the OSNR based on lossless polarization attraction", submitted to Fotonica 2013, Milano, 21-23 maggio 2013.

[2] M. Barozzi, A. Vannucci, and D. Sperti, "Lossless polarization attraction simulation with a novel and simple counterpropagation algorithm for optical signals", *J. Europ. Opt. Soc. : Rap. Pub. (JEOS-RP)*, Vol. 7, 2012, pp. 12042.1-6.

[3] V. V. Kozlov, M. Barozzi, A. Vannucci, and S. Wabnitz, "Lossless polarization attraction of copropagating beams in telecom fibers", *J. Opt. Soc. Am. B (JOSA-B)*, Vol. 30, N. 2, february 2013.

[4] V. V. Kozlov, J. Fatome, P. Morin, S. Pitois, G. Millot, and S. Wabnitz, "Nonlinear repolarization dynamics in optical fibers: transient polarization attraction", *J. Opt. Soc. Am. B (JOSA-B)*, Vol. 28, N. 8, 2011, pp. 1782–1791.

[5] M. Barozzi and A. Vannucci, "Performance analysis of lossless polarization attractors," in Latin America Optics and Photonics Conference, OSA Technical Digest (online) (Optical Society of America, 2012), LM3C.4.

[6] A. Vannucci, A. Bononi, A. Orlandini, E. Corbel, J.-P. Thièry, S. Lanne, and S. Bigo, "Studio analitico e sperimentale dell'impatto del XPM sul grado di polarizzazione (DOP) in sistemi WDM", in Fotonica 2003, Riva del Garda, 7-9 aprile 2003, A3.5.